Physiologia Plantarum
An International Journal for Plant Biology
Physiologia Plantarum 172: 1439–1451. 2021

Reduced photosynthesis in *Arabidopsis thaliana atpme17.2* and *atpae11.1* mutants is associated to altered cell wall composition

Margalida Roig-Oliver[a,*], Catherine Rayon[b], Romain Roulard[b], François Fournet[b], Josefina Bota[a] and Jaume Flexas[a]

[a]Research Group on Plant Biology under Mediterranean Conditions, Departament de Biologia, Universitat de les Illes Balears (UIB) – Agro-Environmental and Water Economics Institute (INAGEA), Palma 07122, Spain
[b]EA 3900-BIOPI, Biologie des Plantes et Innovation, Université de Picardie Jules Verne, Amiens 80039, France

Correspondence
*Corresponding author,
e-mail: margaroig93@gmail.com

Received 28 May 2020
revised 31 July 2020

doi:10.1111/ppl.13186

The cell wall is a complex and dynamic structure that determines plants' performance by constant remodeling of its compounds. Although cellulose is its major load-bearing component, pectins are crucial to determine wall characteristics. Changes in pectin physicochemical properties, due to pectin remodeling enzymes (PRE), induce the rearrangement of cell wall compounds, thus, modifying wall architecture. In this work, we tested for the first time how cell wall dynamics affect photosynthetic properties in *Arabidopsis thaliana* pectin methylesterase *atpme17.2* and pectin acetylesterase *atpae11.1* mutants in comparison to wild-type Col-0. Our results showed maintained PRE activities comparing mutants with wild-type and no significant differences in cellulose, but cell wall non-cellulosic neutral sugars contents changed. Particularly, the amount of galacturonic acid (GalA) – which represents to some extent the pectin cell wall proportion – was reduced in the two mutants. Additionally, physiological characterization revealed that mutants presented a decreased net CO_2 assimilation (A_N) because of reductions in both stomatal (g_s) and mesophyll conductances (g_m). Thus, our results suggest that *atpme17.2* and *atpae11.1* cell wall modifications due to genetic alterations could play a significant role in determining photosynthesis.

Introduction

The plant cell wall is a complex structure surrounding plant cells that determines plant morphology by defining cells' shape and size due to the maintenance of an appropriated turgor pressure (Cosgrove 2005, Ali and Traas 2016). It is mainly composed of cellulose microfibrils cross-linked to non-cellulosic polysaccharides, hemicelluloses. This network consisting of cellulose and hemicelluloses is embedded in a matrix of pectins, another specific type of non-cellulosic polysaccharides

Abbreviations – AE, acetylesterase; A_N, net CO_2 assimilation; C_i, CO_2 concentration at the sub-stomatal cavity; CWPE, cell wall protein extract; DCW, dry cell wall; ETR, electron transport rate; f_{ias}, fraction of mesophyll intercellular air spaces; GalA, galacturonic acid; g_m, mesophyll conductance; g_s, stomatal conductance; HG, homogalacturonans; N_{PAL}, number of palisade layers; PAE, pectin acetylesterase; PME, pectin methylesterase; PRE, pectin remodeling enzymes; RG-I, rhamnogalacturonan type 1; RG-II, rhamnogalacturonan type 2; R_{light}, light respiration; T_{LE}, lower epidermis thickness; T_{LEAF}, leaf thickness; T_{MES}, mesophyll thickness; T_{UE}, upper epidermis thickness; WUE_i, intrinsic water use efficiency; XGA, xylogalacturonan.

(Carpita and Gibeaut 1993, Carpita and McCann 2002, Cosgrove 2005, Lampugnani et al. 2018). By constant remodeling of its components and because of the action of cell wall remodeling enzymes, the cell wall is a highly dynamic structure for the synthesis of new polysaccharides during cell elongation and differentiation and/or in response to stress (Carpita and McCann 2002, Cosgrove 2005, 2016, Tenhaken 2015, Hocq et al. 2017, Kong et al. 2019, Rui and Dinnery 2019).

Although cell wall mechanical properties are often related to the interaction between cellulose and hemicelluloses (Baskin 2005, Geitmann and Ortega 2009), the importance of pectins physicochemical modifications in determining cell wall traits during plants growth and in response to biotic and abiotic stresses – for instance, porosity, hydric status and elasticity – has also been demonstrated (Cosgrove 2005, 2016, Pelloux et al. 2007, Moore et al. 2008, Solecka et al. 2008, McKenna et al. 2010, Gou et al. 2012, Palin and Geitmann 2012, Turbant et al. 2016, Hocq et al. 2017, Kong et al. 2019, Roig-Oliver et al. 2020). Pectins are complex non-cellulosic polysaccharides rich in galacturonic acid (GalA) that can be divided into four main polymers according to their chemical structure: rhamnogalacturonans types 1 and 2 (RG-I and RG-II, respectively), homogalacturonans (HG) and xylogalacturonan (XGA) (Caffall and Mohnen 2009, Atmodjo et al. 2013). Although the ratio between these polysaccharides depends on species, tissues and plant developmental stages, HG are the most abundant ones and consist in linear regions of up to 200 α-1,4-linked GalA residues (Carpita and McCann 2002, Caffall and Mohnen 2009) secreted to the cell wall in a highly methyl-esterified form (70–80%; Pelloux et al. 2007, Guénin et al. 2017). Pectin methylesterases (PME, EC 3.1.1.11) are enzymes which remove HG methyl groups (Pelloux et al. 2007, Turbant et al. 2016, Guénin et al. 2017). Whilst low levels of PME activity have been related to an increase of cell wall rigidity and to alterations in seed germination, plant growth and reproduction (Parre and Geitmann 2005, Bosch and Hepler 2005, Derbyshire et al. 2007, Pelletier et al. 2010, Müller et al. 2013, Leroux et al. 2015, Levesque-Tremblay et al. 2015, Scheler et al. 2015, Turbant et al. 2016, Guénin et al. 2017), enhanced PME activity could lead to cell wall loosening (Peaucelle et al. 2008, 2011). On the other hand, pectin acetylesterases (PAE, EC 3.1.1.6) control the pectin acetylesterification status by regulating the degree of GalA acetylation in both HG and RG-I residues, which can also interfere with plants growth and development (Gou et al. 2008, 2012, de Souza et al. 2014, de Souza and Pauly 2015). However, little is still known regarding the specific biological implications of different acetylation degrees (Gou et al. 2012, de Souza et al. 2014, de Souza and Pauly 2015, Philippe et al. 2017). Thus, the action of pectin remodeling enzymes (PRE) – which includes PME and (P)AE activities – involves changes in pectins physicochemical properties that confer them the ability to rearrange the pectin matrix as well as to modify their interaction between other cell wall compounds modifying wall architecture, thickness and porosity (Cosgrove 2005, Solecka et al. 2008, de Souza and Pauly 2015, Houston et al. 2006, Turbant et al. 2016, Hocq et al. 2017, Kong et al. 2019, Rui and Dinnery 2019). Some of these cell wall characteristics, particularly thickness and porosity, have actually been identified as key traits determining mesophyll conductance (g_m) and, thus, photosynthesis (Terashima et al. 2001, Evans et al. 2009, Flexas et al. 2012, Tomás et al. 2013, Carriquí et al. 2015, 2019, 2020, Tosens et al. 2016, Onoda et al. 2017, Peguero-Pina et al. 2017, Veromann-Jürgenson et al. 2017). As these cell wall characteristics are likely influenced by dynamic changes in its composition, cell wall components rearrangements have been recently shown to affect g_m at an interspecific level under non-stress conditions (Carriquí et al. 2020) and at an intraspecific level in response to environmental stresses (Clemente-Moreno et al. 2019, Roig-Oliver et al. 2020).

The use of mutants has demonstrated that cell wall modifications could involve changes in photosynthesis. Particularly, Ellsworth et al. (2018) tested *Oryza sativa* mutants with disruptions in cell wall mixed-linkage glucan biosynthesis leading to slower growth and phenotypic disruptions such as thinner stems with reduced flexibility. Additionally, Zhang et al. (2020) tested other mutants of the same species in which cellulose microfibrils orientation was disrupted affecting plant growth and photosynthesis as shown by a lower chlorophyll content. Although these studies demonstrate that cell wall modifications alter photosynthesis, their results are difficult to extrapolate to the rest of angiosperms as monocots present specific cell wall composition (Carpita and McCann 2002, Pooper and Tuohy 2010, Sørensen et al. 2010). Thus, the use of *Arabidopsis thaliana* L. (Heynh) as a model plant is more adequate for a better understanding of how cell wall modifications affect photosynthesis. After the completion of its genome sequence (Arabidopsis Genome Initiative 2000), *Arabidopsis* has gained importance because it is relatively easy to generate mutants to study how specific genetic alterations modify both biochemical and physiological processes. Although Weraduwage et al. (2016) have already tested *A. thaliana* mutants with alterations in pectin methyltransferases showing that they changed both PME activity and photosynthesis, further information regarding other relevant enzyme activities – such as pectin acetylesterases – is necessary for a better understanding of how

cell wall dynamics can affect photosynthesis, especially g_m. Thus, we provide a study in which *A. thaliana atpme17.2*, a type I PME (Sénéchal et al. 2014), and *atpae11.1* (Philippe et al. unpublished) mutants were tested for the first time in comparison to wild-type Col-0 in order to evaluate the role of cell wall composition and PRE activities in determining photosynthetic efficiency.

Materials and methods

Plant material and growth conditions

A. thaliana atpme17.2 (SALK_059908) and *atpae11.1* (GK 505H02) mutants from wild-type Columbia (Col-0) were isolated from SALK (SIGnAL, USA) and GABI (CeBiTec, Germany) T-DNA insertion collections, respectively, using gene-specific forward and reverse primers and T-DNA left border specific primers (Sénéchal et al. 2014, Philippe et al. unpublished data). Whilst the T-DNA insertion was localized in the first intron for *atpme17.2*, it was localized in the tenth for *atpae11.1*. Twelve seeds of each studied genotype were sown individually in horticultural alveolus with a substrate mixture containing peat and perlite (3:1, v/v). Horticultural alveolus with plastic trays for sub-irrigation were placed in a growth chamber at 22°C with 12/12 h light/darkness daily fluctuation receiving 200–250 μmol m^{-2} s^{-1} photosynthetic photon flux density (PPFD) and they were watered three times per week with Hoagland solution 50%. Three weeks later, six individual replicates per genotype were randomly selected to be transplanted to individual pots filled with the same substrate mixture following the 'ice-cream cone-like' method (Flexas et al. 2007a). Thus, plants grew with their bases on the top of the 'cone', with their rosette spreading downwards to facilitate gas-exchange measurements. In all cases, plants were subjected to these conditions for 40 days.

Gas-exchange and fluorescence measurements

Forty days after the sowing, a fully developed leaf per plant from the third to last pair of the rosette was selected for simultaneous gas-exchange and chlorophyll *a* fluorescence (Chl *a*) measurements using an infrared gas analyzer (IRGA) LI-6400XTR equipped with a fluorometer (Li-6400-40; Li-Cor Inc.). Measurements were performed from 09:00 to 15:00 h. Leaves were clamped into a 2 cm^2 cuvette. The block temperature was kept at 25°C and the vapor pressure deficit (VPD) at around 1.5 kPa. Leaf steady-state conditions were induced at saturating photosynthetic photon flux density (PPFD 1250 μmol m^{-2} s^{-1}, 90–10% red-blue light) and 400 μmol CO_2 mol^{-1} air. The flow rate was fixed at 300 μmol air min^{-1}. When steady-state conditions were reached, A_N-C_i curves were performed increasing ambient CO_2 concentrations (C_a) from 50 to 1500 μmol CO_2 mol^{-1} air. Measurements for net CO_2 assimilation (A_N), stomatal conductance (g_s), CO_2 concentration at the sub-stomatal cavity (C_i) and steady-state fluorescence (F_s) were registered after the stabilization of the gas-exchange rates in a given C_a in a period comprised between 180 and 240 s. Then, a saturating light flash was applied to obtain the maximum fluorescence (F_m'). From these values, the real quantum efficiency of photosystem II (Φ_{PSII}) was registered. All A_N-C_i data was corrected for CO_2 leakage in and out of the IRGA chamber following Flexas et al. (2007b). Light curves under non-photorespiratory conditions were assessed as described in Valentini et al. (1995) to calculate the electron transport rate (ETR). Light respiration (R_{light}) was assumed as half the dark respiration rate, determined after plants exposure to full darkness for, at least, 20 min (Niinemets et al. 2005). From all these parameters, mesophyll conductance (g_m) was calculated according to Harley et al. (1992) using the value for CO_2 compensation point in the absence of respiration (Γ^*) reported by Whitney et al. (2011) for *A. thaliana*.

Anatomical measurements

After gas-exchange measurements, one randomly selected plant per genotype was used to collect samples for anatomy. Thus, small pieces of those leaves used for gas-exchange measurements were cut avoiding main foliar structures and were fixed under vacuum pressure with glutaraldehyde 4% and paraformaldehyde 2% in a 0.01 M phosphate buffer (pH 7.4). Afterward, they were post-fixed in 2% buffered osmium tetroxide for 2 h and dehydrated by a graded ethanol series. Obtained pieces were embedded in LR white resin (London Resin Company) and were placed in an oven at 60°C for 48 h (Tomás et al. 2013, Carriquí et al. 2015, 2019). Semi-fine (0.8 μm) cross-sections were cut with an ultramicrotome (Leica RM2265, Leica Biosystems) and were stained with toluidine blue 0.1% to be observed in bright field with a light microscope (Nikon-Eclipse-90i). Pictures at ×100 magnifications were taken to determine leaf thickness (T_{LEAF}), upper epidermis thickness (T_{UE}), lower epidermis thickness (T_{LE}), mesophyll thickness (T_{MES}), number of palisade layers (N_{PAL}) and fraction of mesophyll intercellular air spaces (f_{ias}). Values for all parameters were obtained as an average of 10 measurements from randomly selected cell structures using the ImageJ software (Wayne Rasband/NIH).

Cell wall composition

Sampling for cell wall analysis was performed in those leaves adjacent to the one used for gas-exchange measurements after leaving plants under dark conditions overnight to minimize starch content. Around 0.5–1 g of fresh leaf tissue per plant were frozen in liquid nitrogen, freeze-dried, ground to fine powder in a ball mill and stored at −80°C. Plant cell wall material was prepared from 10 mg of dry leaf powder according to Peña et al. (2004). Dry cell wall material (DCW) was digested with α-amylase according to Fleischer et al. (1999). Following Foster et al. (2010), 3 mg of each α-amylase-digested DCW were placed in screw-capped glass tubes to be hydrolysed with 1 ml of 2 N trifluoroacetic acid at 100°C for 90 min, cooled down at room temperature and centrifuged obtaining two phases: the supernatant (non-cellulosic cell wall sugars, i.e. hemicelluloses and pectins) and the pellet (cellulosic cell wall sugars). Trifluoroacetic acid remains from the supernatant were evaporated under nitrogen flow to quantify specific neutral sugars from hemicelluloses cell wall fraction (i.e. fucose, rhamnose, arabinose, galactose, glucose, xylose and mannose) and from pectin fraction (i.e. galacturonic acid) as described in Turbant et al. (2016). After evaporated, hydrolysates were dissolved with 1 ml of deionized water and each one was diluted (1:10, v/v) to determine its specific non-cellulosic neutral sugars composition by high-performance anion-exchange chromatography coupled with a pulsed electrochemical detection (HPAEC-PAD; Dionex ICS-3000, Dionex Corporation).

Cellulose content was estimated following Foster et al. (2010). Thus, pellets were cleaned three times with deionized water and subsequently freeze-dried overnight. Freeze-dried samples were resuspended in 1 ml Updegraff reagent (acetic acid: nitric acid: deionized water, 8:1:2 v/v) to be heated at 100°C for 30 min. Once cooled, samples were centrifuged at 10 000 *g* and pellets were cleaned twice with deionized water and three times with absolute acetone. Then, they were freeze-dried overnight. The following morning, 175 µl sulfuric acid 72% were added and samples were incubated at 30°C for 45 min. Afterward, 825 µl deionized water was added and the mixtures were centrifuged at 10 000 *g*. Finally, 200 µl anthrone reagent prepared in sulfuric acid 100% (2:1, w:v) plus 90 µl deionized water was added to 10 µl of each supernatant. Samples absorbance was read at 625 nm using a Microplate Spectrophotometer (BioTek PowerWave). Cellulose concentration was determined by interpolating samples absorbance from a glucose calibration curve.

Protein extraction and cell wall enzyme activity assays

Enriched weakly bound cell wall proteins (CWP) were extracted to perform PME and (P)AE enzyme activities assays. Briefly, around 0.7–1 g fresh leaf tissue from leaves adjacent to the one used for gas-exchange measurements were sampled, grounded to fine powder using a ball mill and stored at −80°C. Then, 50 mg of frozen plant powder were homogenized in 150 µl of 50 mM sodium dihydrogen phosphate (pH 7.5) containing 2 M sodium chloride. Samples were incubated at 4°C under constant agitation for 30 min before centrifugation at 13 000 *g*. The supernatants were recovered and a second extraction was performed on pellets following the same methodology. The supernatants were combined and desalted on Amicon Ultra-0.5 Centrifugal Filter Unit 3Kda cut-off (Merck Millipore) using McIlvaine buffer (0.2 M disodium hydrogen phosphate prepared in 0.1 M citric acid, pH 6.5) containing 100 mM sodium chloride. Protein concentration was determined according to Bradford (1976). Thus, samples absorbance was read at 595 nm using a spectrophotometer (BioTek PowerWave) and CWP concentration was determined by interpolating samples values from a bovine serum albumin calibration curve.

The overall PME enzyme activity was determined by measuring the methanol released from pectin methyl ester content (Baldwin et al. 2014). Briefly, 5 µl of each CWP were incubated with 85 µl of 50 mM sodium phosphate buffer (pH 7.5) containing 0.025 U alcohol oxidase and 100 µg methyl-esterified citrus pectin solution 90%. Samples were incubated at 28°C for 30 min and, then, 100 µl of staining solution (2 M ammonium acetate and 20 mM pentane-2,4-dione prepared in 50 mM glacial acetic acid) were added. They were incubated at 68°C under darkness conditions for 15 min and their absorbance was read at 420 nm with a spectrophotometer (BioTek PowerWave). PME enzyme activity was determined by interpolating samples values from a methanol calibration curve.

AE and PAE enzyme activities were estimated by measuring acetate release using triacetin and sugar beet as a substrate, respectively (Baldwin et al. 2014, Remoroza et al. 2014). Thus, 20 µg of CWP extract in a final volume of 30 µl were incubated with 0.2 M sodium dihydrogen phosphate prepared in 100 mM sodium chloride and 0.1 M citric acid (pH 6.5). Then, 120 µl of 100 mM triacetin (Sigma) or 10 mg ml^{-1} of sugar beet pectin (42% methylesterification and 31% acetylation degrees, CP Kelco) prepared in McIlvaine buffer containing 100 mM sodium chloride were added to samples for AE or PAE assays, respectively. They were incubated at 40°C under

constant agitation for 2 h. Once cooled, the acetate concentration of each sample was determined with the Acetic Acid Kit (Megazyme, K-ACETRM). Samples absorbance was read at 340 nm with a spectrophotometer (BioTek PowerWave). AE and PAE enzyme activities were determined by interpolating samples values from an acetic acid calibration curve.

Statistical analysis

Thompson test was performed to detect and eliminate outliers for all tested parameters. Then, one-way ANOVA and subsequent LSD test were assessed to detect statistically significant differences for the studied parameters between genotypes ($P < 0.05$). All analyses were performed with R software (ver. 3.2.2; R Core Team, Austria).

Results

Pectin remodeling enzymes activities

No significant changes in PRE activities were observed comparing *atpme17.2* and *atpae11.1* mutants with the wild-type Col-0 (Fig. 2). Particularly, all tested genotypes presented similar amount of PME enzyme activity (0.18 ± 0.01, 0.19 ± 0.02 and 0.18 ± 0.01 nmol methanol μg protein^{-1} min^{-1} for Col-0, *atpae11.1* and *atpme17.2*, respectively; Fig. 2A). A similar pattern was detected for both AE and PAE enzyme activities (Fig. 2B,C, respectively).

Cell wall cellulosic and non-cellulosic sugars characterization

Cellulose content did not differ between the studied genotypes (Fig. 3A). However, there was a strong reduction in the cell wall pectin fraction, expressed by the amounts of galacturonic acid, in both *atpae11.1* and *atpme17.2* mutants (34.55 ± 3.96 and 66.27 ± 5.78 % WT, respectively; Fig. 3A). Regarding the hemicellulosic cell wall fraction, although both mutants presented increased fucose content in comparison to Col-0, these changes were only significant for *atpae11.1* (Fig. 3B). Nonetheless, no significant modifications were detected comparing the amount of other non-cellulosic neutral sugars belonging to hemicelluloses (i.e. rhamnose, arabinose, galactose, glucose, xylose and mannose) among genotypes (Fig. 3B).

Photosynthetic characterization

The analysis of A_N-C_i curves revealed that both *atpae11.1* and *atpme17.2* mutants showed strong reductions in photosynthetic capacity accompanied by diminished C_i (Supporting Information, Fig. S1). At ambient CO_2 concentration, mutants presented more than a two-fold decrease in A_N compared to wild-type (4.95 ± 1.19, 3.24 ± 0.58 and 10.05 ± 0.63 μmol CO_2 m^{-2} s^{-1} for *atpae11.1*, *atpme17.2* and Col-0, respectively; Fig. 4A). Additionally, decreases in g_s were also detected, being more pronounced in *atpme17.2* (0.11 ± 0.02 mol CO_2 m^{-2} s^{-1}; Fig. 4B). However, these A_N and g_s reductions in both mutants did not lead to differing WUE_i in comparison to Col-0 (Fig. 4C). Again, g_m reductions were found in both mutants, especially in *atpme17.2* with a g_m eight-fold lower than Col-0 (Fig. 4D). Finally, no significant differences among genotypes were found for ETR and R_{light} (Fig. 4E,F, respectively).

Anatomical characterization

The preliminary analysis of leaf anatomic features indicated a reduction in T_{LEAF} which was observed in both mutants in comparison to Col-0 (Table S1). However, they presented slightly increased and reduced T_{UE} and T_{LE}, respectively, than the wild-type (Table S1). Additionally, in both mutants there were indications of a decrease in T_{MES}, but even more marked in *atpae11.1*, which also obtained lower N_{PAL} than Col-0 (Table S1). Finally, changes in f_{ias} suggested an increase of porosity in *atpme17.2* and *atpae11.1* in comparison to Col-0 (Table S1).

Discussion

Cell wall rearrangement is an important feature determining plants' development during their entire life (Carpita and McCann 2002, Cosgrove 2005, 2016, Tenhaken 2015, Hocq et al. 2017, Lampugnani et al. 2018, Kong et al. 2019, Rui and Dinnery 2019). In this work, *A. thaliana atpme17.2* and *atpae11.1* mutants were studied in comparison to wild-type Col-0 to assess for the first time whether potential differences in their cell wall composition – including PRE activities – could affect photosynthesis.

Several studies have evidenced phenotypic effects occurring in specific *Arabidopsis* mutants (for instance, Hernández-Blanco et al. 2007, Kong et al. 2014, López-Calcagno et al. 2017, Zhao et al. 2018), which were also detected in this study as mutant plants reduced their rosette diameter as well as their foliar size in comparison to wild-type (Fig. 1). In fact, alterations of PRE activities could be involved in several physiological processes due to the remodeling of cell wall architecture, which could modify the plants' phenotype (Carpita and McCann 2002, Cosgrove 2005, 2016, Hocq et al. 2017, Kong et al. 2019). Particularly, the effects of altered PME have been widely studied and, in *Arabidopsis*, they are implicated in seed germination (Müller et al. 2013),

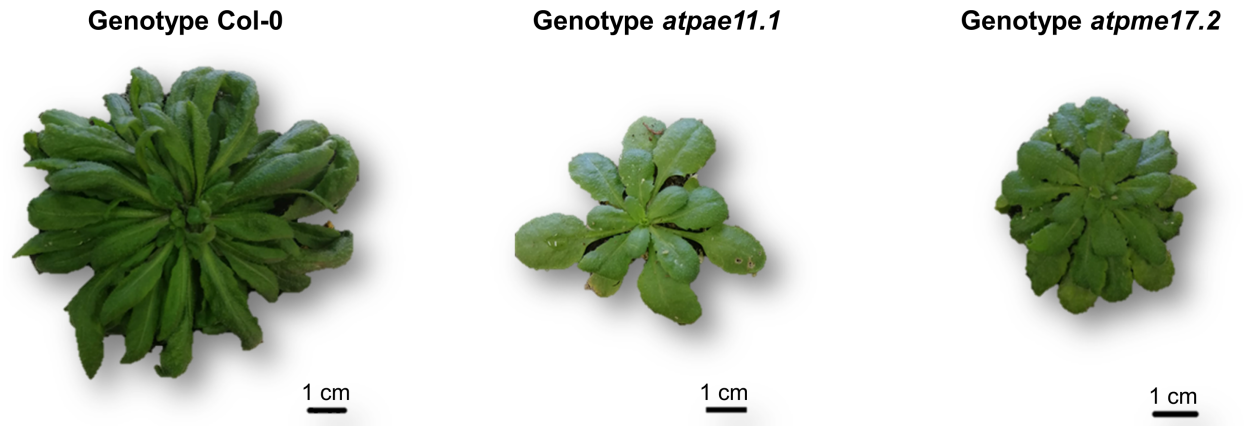

Fig. 1. Representative phenotypical alterations of 40-day-old wild-type Col-0 in comparison to *atpae11.1* and *atpme17.2* mutant genotypes.

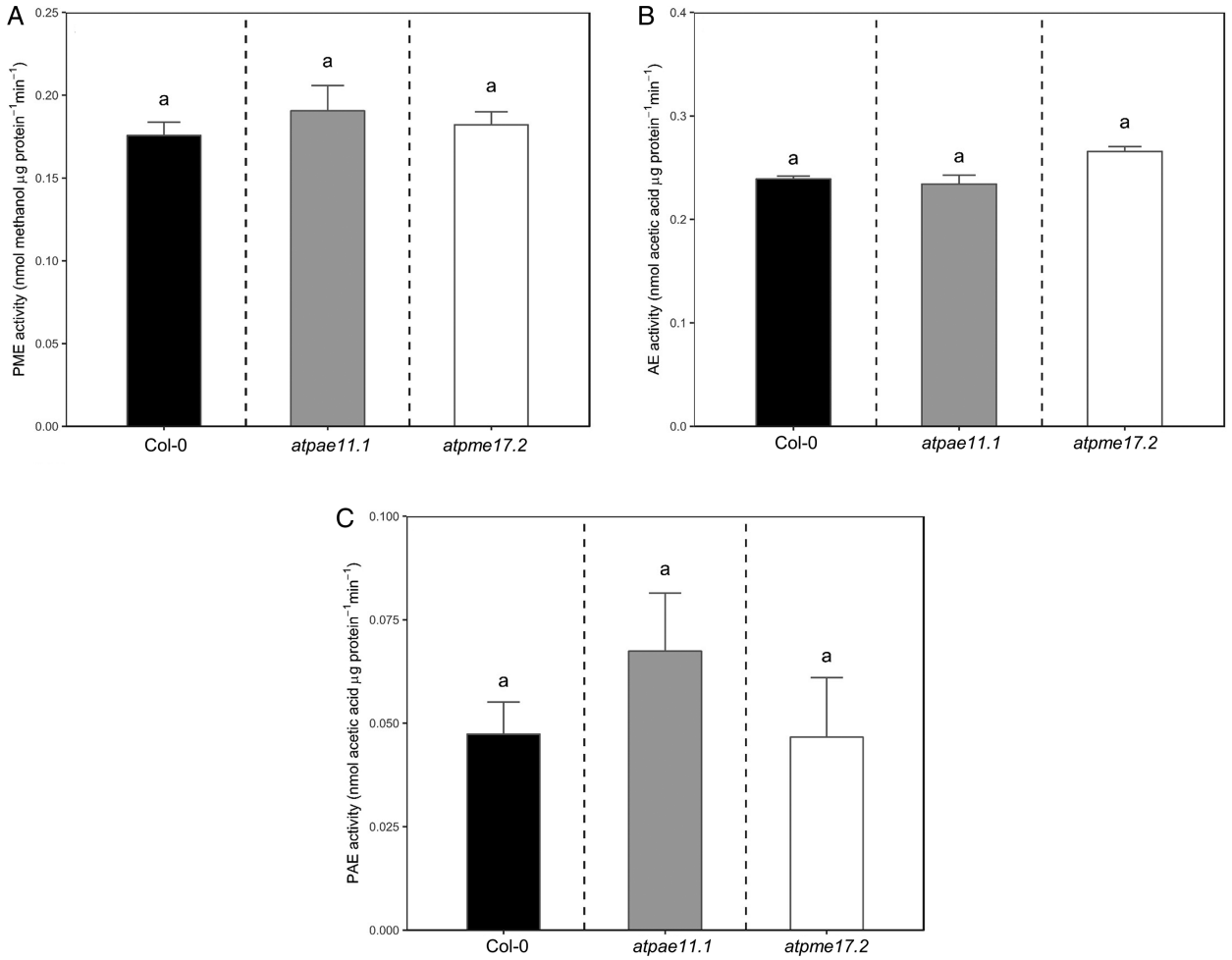

Fig. 2. Enzyme activities in *Arabidopsis thaliana* Col-0, *atpae11.1* and *atpme17.2* genotypes. (A) Pectin methylesterase, (B) acetylesterase and (C) pectin acetylesterase. Different superscript letters indicate significant difference ($P < 0.05$) between genotypes according to LSD test. n = 4–6 (means ± SE).

seed mucilage adhesion (Turbant et al. 2016), reduction of root hair production (Guénin et al. 2017), pollen grain maturation and germination (Leroux et al. 2015), dark-grown hypocotyls (Derbyshire et al. 2007, Pelletier et al. 2010) or even in stomatal function (Amsbury et al. 2016). On the other hand, although there is limited information regarding specific biological effects of PAE on plants growth and development, it seems that it could be involved in determining *Arabidopsis* inflorescence stem height (de Souza et al. 2014) and in regulating pollen tube growth and plant reproduction in other species (Gou et al. 2012). However, we did not observe any significant differences in PRE activities comparing mutant genotypes with Col-0 (Fig. 2). Although Sénéchal et al. (2014) and Philippe et al. (unpublished data) reported that *AtPME17* and *AtPAE11*, respectively, were highly expressed in older leaves and roots, there is no obvious correlation between high transcript levels and translation into high protein levels and/or high enzymes activities (Bosch and Hepler 2005, Jamet et al. 2009). Additionally, although *atpme17.2* and *atpae11.1* exhibited mutations in the same genes than those mutants used in Sénéchal et al. (2014) and Philippe et al. (unpublished data), the ones studied here presented alterations in introns, while those used in the above-mentioned studies were localized in exons. Thus, we suggest that different positions of the T-DNA insertions used for our mutant genotypes could be involved in differing PRE activities in comparison to previous reports. Furthermore, our tested mutants could contain specific PME and/or PAE proteins which may not be present in Col-0, thus, compensating PME and PAE activities. In *A. thaliana*, pectin methylesterases belong to a multigenic family of 66 isoforms (Pelloux et al. 2007). Therefore, as it has been proposed that some genes could control the same processes (Bosch and Hepler 2005), those alterations related to *AtPME17.2* could be supplied for other similar or related genes. Similarly, pectin acetylesterases belong to a multigenic family of 12 isoforms in *A. thaliana*, but their implications are not fully understood (Gou et al. 2012, Philippe et al. 2017). For instance, de Souza et al. (2014) reported a genetic characterization of null *atpae8* and *atpae9* mutants showing that they presented 20% more acetate in their cell wall. Moreover, the double mutant showed an even more enhanced acetate cell wall proportion (37%). However, Orfila et al. (2012) overexpressed an ortholog *Arabidopsis AtPAE8* from *Vigna unguiculata* in potato and found a decreased degree of pectin acetylation. Following previous studies, we expected changes in PAE activity, but it was maintained at similar levels in all tested genotypes perhaps due to genetic redundancy.

Despite enzymatic activities were maintained, the two mutants presented alterations of cell wall composition which could explain the phenotypic differences. However, our results for cell wall non-cellulosic neutral sugars analyses differed from previous reports by Mertz et al. (2012) and Engelsdorf et al. (2017). Particularly, Mertz et al. (2012) determined that galacturonic acid (GalA) was the most abundant non-cellulosic neutral sugar in *A. thaliana mur* mutants. Additionally, Engelsdorf et al. (2017) tested *A. thaliana pgm*, *adg1-1* and *sex1-1* mutants and showed that neutral sugars from the hemicellulosic cell wall fraction significantly changed in comparison to wild-type Col-0, whilst GalA amounts were maintained. Nonetheless, our results differed from the previous studies probably because, apart from testing

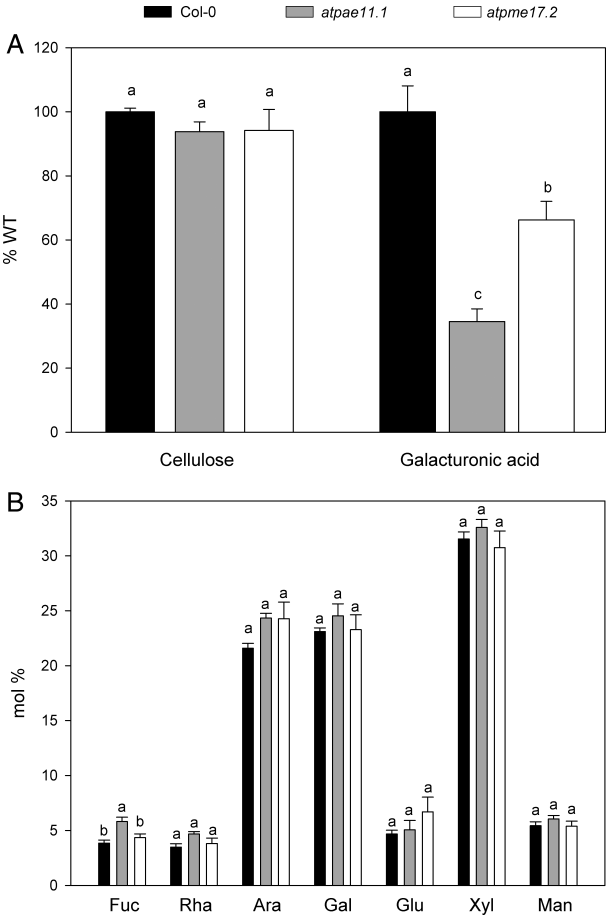

Fig. 3. Cell wall composition of *A. thaliana* Col-0, *atpae11.1* and *atpme17.2* genotypes. (A) Cellulose and galacturonic acid content and (B) non-cellulosic neutral sugars content from hemicellulosic cell wall fraction: L-fucose (Fuc), L-rhamnose (Rha), L-arabinose (Ara), D-galactose (Gal), D-glucose (Glu), D-xylose (Xyl) and D-mannose (Man). Different superscript letters indicate significant difference ($P < 0.05$) between genotypes according to LSD test. n = 4–6 (means ± SE).

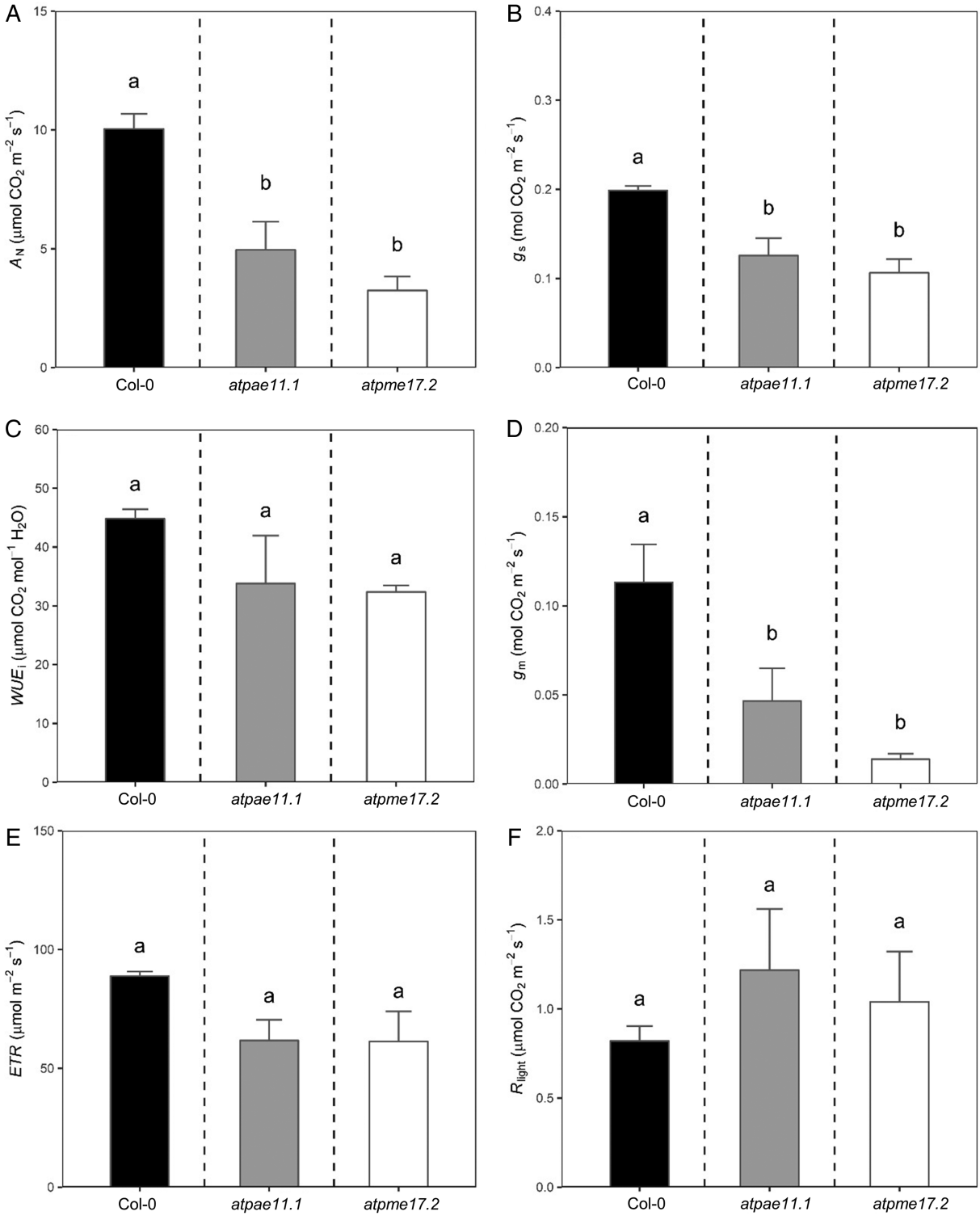

Fig. 4. Photosynthetic characterization of *A. thaliana* Col-0, *atpae11.1* and *atpme17.2* genotypes. (A) Net CO_2 assimilation (A_N), (B) stomatal conductance (g_s), (C) intrinsic water use efficiency (WUE_i), (D) mesophyll conductance (g_m), (E) electron transport rate (ETR) and (F) light respiration (R_{light}). Different superscript letters indicate significant difference ($P < 0.05$) between genotypes according to LSD test. n = 5–6 (means ± SE).

other mutants, our plants were grown under different conditions, for instance, different photoperiod, light intensity and soil composition. Additionally, we performed the trifluoroacetic acid hydrolysis at 100°C instead of at 121°C, which may have resulted in higher resistance to the acid hydrolysis of the linkages between GalA-GalA and rhamnose-GalA, thus, obtaining lower amounts of both non-cellulosic neutral sugars than expected. However, our results showed that both mutants experienced decreased amounts of GalA (i.e. pectins) compared to wild-type (Fig. 3A) with maintained PRE activities. In fact, there is no obvious correlation between altered PRE activities and modified pectins quantity probably because they determine pectins physicochemical properties, not their amount (Pelloux et al. 2007, Gou et al. 2012, Palin and Geitmann 2012, Turbant et al. 2016, Hocq et al. 2017, Kong et al. 2019). Therefore, this descent in pectins as well as some additional mutant-specific alterations in the hemicellulosic cell wall fraction such as increased fucose in *atpae11.1* (Fig. 3B), could explain the diminished photosynthetic capacity (Figs 4 and S1) as previously reported (Weraduwage et al. 2016), especially, via altered g_m (Ellsworth et al. 2018, Clemente-Moreno et al. 2019, Carriquí et al. 2020, Roig-Oliver et al. 2020). Of the previous studies, Clemente-Moreno et al. (2019) and Roig-Oliver et al. (2020) demonstrated a cell wall composition-mediated effect on g_m based on correlative evidence after stress-inducing changes in both g_m and cell wall composition testing tobacco and grapevines, respectively. Particularly, Clemente-Moreno et al. (2019) found a negative relationship between non-cellulosic sugars, specifically pectins, with g_m. Although Weraduwage et al. (2016) did not focus on modifications of g_m, they also highlighted the importance of pectins as possible drivers of altered photosynthesis in *A. thaliana* cell wall mutants. However, only Ellsworth et al. (2018) used cell wall mutants to directly demonstrate the role of cell wall composition on g_m. Specifically, they used rice mutants with disruptions in cell wall mixed-linkage glucan – a compound specific of grasses – production and showed a reduction in g_m of 83%, which was only partially explained by changes in observed anatomical properties. In fact, Weraduwage et al. (2016) also reported that anatomical alterations derived from cell wall modifications were important determinants of photosynthesis. The results provided in these previous studies lead to the suggestion that altered cell wall composition may induce changes in cell wall effective porosity and CO_2 diffusion path length and/or chemical properties, thus, changing photosynthesis. Nonetheless, our results follow a different pattern than those reported by Clemente-Moreno et al. (2019) probably because they only tested one single genotype after short-term water and salt stresses induction. As our tested genotypes were grown under non-stressing conditions and the observed phenotypical differences are likely to be constitutive, we believe that our data on *atpme17.2* and *atpae11.1* mutants could be much more comparable with that from Carriquí et al. (2020). Particularly, while they demonstrated that pectins themselves did not correlate with g_m testing seven conifers species, they found a strong positive relationship between g_m and the ratio of pectins to celluloses and hemicelluloses. Even though in this study we do not have enough data to calculate this ratio, the fact that celluloses were equally maintained among genotypes, and pectins were not, suggests that g_m reductions in *atpme17.2* and *atpae11.1* mutants could also be related to a diminished fraction of pectins to celluloses and, perhaps, hemicelluloses. Additionally, although anatomical traits were studied only preliminarily in this work, we hypothesize that together with non-cellulosic sugars alterations they could also be involved in photosynthesis reduction in both mutants as they display, for instance, decreased T_{LEAF} and T_{MES} as compared to wild-type (Table S1). However, more detailed anatomical studies of *atpme17.2* and *atpae11.1* mutants using more replicates would be necessary to confirm this point. Finally, and contrary to Ellsworth et al. (2018), the mutants also showed a significant decrease of g_s (although of lower magnitude than that of g_m). Whether this is an indirect consequence of co-adjustment with reduced g_m (Flexas et al. 2013) or a direct effect of cell wall composition on stomata (Jones et al. 2003) remains to be elucidated.

This study provides insights on how different cell wall architecture could influence the photosynthetic efficiency in *A. thaliana atpme17.2* and *atpae11.1* mutants in comparison to wild-type Col-0. Thus, we established that cell wall composition modification could lead to reduced photosynthetic traits in *atpme17.2* and *atpae11.1* mutants maybe because of alterations in leaf chemistry and, perhaps, in anatomical traits. However, more studies are required to establish the potential implications of *AtPME17.2* and *AtPAE11.1* in whole plant dynamics using mutants where the T-DNA insertion is localized in their specific catalytic sites.

Author contributions

M.R.-O., C.R., J.B. and J.F. designed the study; M.R.-O., C.R., R.R. and F.F. conducted the experiment; M.R.-O. performed the data analysis and M.R.-O., J.B. and J.F. wrote the first manuscript version. All authors contributed to its following versions.

Acknowledgements – This work was supported by the project PGC2018-093824-B-C41 from Ministerio de Economía y Competitividad (MINECO, Spain). M.R.-O. was supported by a predoctoral fellowship FPU16/01544. We thank Ms. Maïté Leschevin for her help during enzymatic activities assays performance.

Data Availability Statement

Data sharing is not applicable to this article as no new data were created or analyzed in this study.

References

Ali O, Traas J (2016) Force-driven polymerization and turgor-induced wall expansion. Trends Plant Sci 21: 398–409

Amsbury S, Hunt L, Elhaddad N, Baillie A, Lundgren M, Verhertbruggen Y, Scheller HV, Knox JP, Fleming AJ, Gray JE (2016) Stomatal function requires pectin de-methyl-esterification of the guard cell wall. Curr Biol 26: 2899–2906

Arabidopsis Genome Initiative (2000) Analysis of the genome sequence of the flowering plant *Arabidopsis thaliana*. Nature 408: 796–815

Atmodjo MA, Zhangying H, Mohnen D (2013) Evolving views of pectin biosynthesis. Annu Rev Plant Biol 64: 747–779

Baldwin L, Domon JM, Klimek JF, Fournet F, Sellier H, Gillet F, Pelloux J, Lejeune-Hénaut I, Carpita NC, Rayon C (2014) Structural alteration of cell wall pectins accompanies pea development in response to cold. Phytochemistry 104: 37–47

Baskin TI (2005) Anisotropic expansion of the plant cell wall. Annu Rev Cell Dev Biol 21: 203–222

Bosch M, Hepler PK (2005) Pectin methylesterases and pectin dynamics in pollen tubes. Plant Cell 17: 3219–3226

Bradford MM (1976) A rapid and sensitive method for the quantitation of microgram quantities of protein utilizing the principle of protein-dye binding. Anal Biochem 72: 248–254

Caffall KH, Mohnen D (2009) The structure, function, and biosynthesis of plant cell wall pectic polysaccharides. Carbohydr Res 344: 1879–1900

Carpita NC, Gibeaut DM (1993) Structural models of primary cell walls in flowering plants: consistency of molecular structure with the physical properties of the walls during growth. Plant J 3: 1–30

Carpita NC, McCann MC (2002) The functions of cell wall polysaccharides in composition and architecture revealed through mutations. Plant and Soil 247: 71–80

Carriquí M, Cabrera HM, Conesa MÀ, Coopman RE, Douthe C, Gago J, Gallé A, Galmés J, Ribas-Carbó M, Tomás M, Flexas M (2015) Diffusional limitations explain the lower photosynthetic capacity of ferns as compared with angiosperms in a common garden study. Plant Cell Environ 38: 448–460

Carriquí M, Roig-Oliver M, Brodribb TJ, Coopman R, Gill W, Mark K, Niinemets Ü, Perera-Castro AV, Ribas-Carbó M, Sack L, Tosens T, Waite M, Flexas J (2019) Anatomical constraints to nonstomatal diffusion conductance and photosynthesis in lycophytes and bryophytes. New Phytol 222: 1256–1270

Carriquí M, Nadal M, Clemente-Moreno MJ, Gago J, Miedes E, Flexas J (2020) Cell wall composition strongly influences mesophyll conductance in gymnosperms. Plant J, 103: 1372–1385. https://doi.org/10.1111/tpj.14806

Clemente-Moreno MJ, Gago J, Díaz-Vivancos P, Bernal A, Miedes E, Bresta P, Liakopoulos G, Fernie AR, Hernández JA, Flexas J (2019) The apoplastic antioxidant system and altered cell wall dynamics influence mesophyll conductance and the rate of photosynthesis. Plant J 99: 1031–1046

Cosgrove DJ (2005) Growth of the plant cell wall. Nat Rev Mol Cell Biol 6: 850–861

Cosgrove DJ (2016) Plant cell wall extensibility: connecting plant cell growth with cell wall structure, mechanics, and the action of wall-modifying enzymes. J Exp Bot 67: 463–476

de Souza AJ, Hull PA, Gille S, Pauly M (2014) Identification and functional characterization of the distinct plant pectin esterases PAE8 and PAE9 and their deletion mutants. Planta 240: 1123–1138

de Souza AJ, Pauly M (2015) Comparative genomics of pectinacetylesterases: insight on function and biology. Plant Signal Behav 10: e1055434

Derbyshire P, McCann MC, Roberts K (2007) Restricted cell elongation in *Arabidopsis* hypocotyls is associated with a reduced average pectin esterification level. BMC Plant Biol 7: 31

Ellsworth PV, Ellsworth PZ, Koteyeva NK, Cousins AB (2018) Cell wall properties in *Oryza sativa* influence mesophyll CO_2 conductance. New Phytol 219: 66–76

Engelsdorf T, Will C, Hofmann J, Schmitt C, Merritt BB, Rieger L, Frenger MS, Marschall A, Franke RB, Pattathil S, Voll LM (2017) Cell wall composition and penetration resistance against the fungal pathogen *Colletotrichum higginsianum* are affected by impaired starch turnover in *Arabidopsis* mutants. J Exp Bot 68: 701–713

Evans JR, Kaldenhoff R, Genty B, Terashima I (2009) Resistance along the CO_2 diffusion pathway inside leaves. J Exp Bot 60: 2235–2248

Fleischer A, O'Neill MA, Ehwald R (1999) The pore size of non-graminaceous plant cell walls is rapidly decreased by borate ester cross-linking of the pectic polysaccharide rhamnogalacturonan II. Plant Physiol 121: 829–838

Flexas J, Ortuño MF, Ribas-Carbó M, Díaz-Espejo A, Flórez-Saraza ID, Medrano H (2007a) Mesophyll conductance to CO_2 in *Arabidopsis thaliana*. New Phytol 175: 501–511

Flexas J, Díaz-Espejo A, Berry JA, Cifre J, Galmés J, Kaldenhoff R, Medrano H, Ribas-Carbó M (2007b) Analysis of leakage in IRGA's leaf chambers of open gas exchange systems: quantification and its effects in photosynthesis parameterization. J Exp Bot 58: 1533–1543

Flexas J, Barbour MM, Brendel O, Cabrera HM, Carriquí M, Díaz-Espejo A, Douthe C, Dreyer E, Ferrio JP, Gago J, Gallé A, Galmés J, Kodama N, Medrano H, Niinemets Ü, Peguero-Pina JJ, Pou A, Ribas-Carbó M, Tomás M, Tosens T, Warren CR (2012) Mesophyll conductance to CO_2: an unappreciated central player in photosynthesis. Plant Sci 193-194: 70–84

Flexas J, Niinemets Ü, Gallé A, Barbour MM, Centritto M, Díaz-Espejo A, Douthe C, Galmés J, Ribas-Carbó M, Rodríguez PL, Rosselló F, Soolanayakanahally R, Tomás M, Wright IJ, Farqujar GD, Medrano H (2013) Diffusional conductances to CO_2 as a target for increasing photosynthesis and photosynthetic water-use efficiency. Photosynth Res 117: 45–59

Foster CE, Martin TM, Pauly M (2010) Comprehensive compositional analysis of plant cell walls (lignocellulosic biomass) part II: carbohydrates. JoVE 37: 1837

Geitmann A, Ortega JKE (2009) Mechanics and modelling of plant cell growth. Trends Plant Sci 14: 467–478

Gou JY, Park S, Yu XH, Miller LM, Liu CJ (2008) Compositional characterization and imaging of "wall-bound" acylesters of *Populus trichocarpa* reveal differential accumulation of acyl molecules in normal and reactive woods. Planta 229: 15–24

Gou JY, Miller LM, Hou G, Yu XH, Chen XY, Liu CJ (2012) Acetylesterase-mediated deacetylation of pectin impairs cell elongation, pollen germination, and plant reproduction. Plant Cell 24: 50–65

Guénin S, Hardouin J, Paynel F, Müller K, Mongelard G, Driouich A, Lerouge P, Kermode AR, Lehner A, Mollet JC, Pelloux J, Gutiérrez L, Mareck A (2017) AtPME3, a ubiquitous cell wall pectin methylesterase of *Arabidopsis thaliana*, alters the metabolism of cruciferin seed storage proteins during post-germinative growth of seedlings. J Exp Bot 68: 1083–1095

Harley PC, Loreto F, Di Marco G, Sharkey TD (1992) Theoretical considerations when estimating the mesophyll conductance to CO_2 flux by the analysis of the response of photosynthesis to CO_2. Plant Physiol 98: 1429–1436

Hernández-Blanco C, Feng DX, Hu J, Sánchez-Vallet A, Deslandes L, Llorente F, Berrocal-Lobo M, Keller H, Barlet X, Sánchez-Rodríguez C, Anderson LK, Somerville S, Marco Y, Molina A (2007) Impairment of cellulose synthase required for *Arabidopsis* secondary cell wall formation enhances disease resistance. Plant Cell 19: 890–903

Hocq L, Sénéchal F, Lefebvre V, Lehner A, Domon JM, Mollet JC, Dehors J, Pageau K, Marcelo P, Guérineau F, Kolšek K, Mercadante D, Pelloux J (2017) Combined experimental and computational approaches reveal distinct pH dependence of pectin methylesterase inhibitors. Plant Physiol 173: 1075–1093

Houston K, Tucker MR, Chowdhury J, Shirley N, Little A (2006) The plant cell wall: a complex and dynamic structure as revealed by the responses of genes under stress conditions. Front Plant Sci 7: 984

Jamet E, Roujol D, San-Clemente H, Irshad M, Soubigou-Taconnat L, Renou JP, Pont-Lezica R (2009) Cell wall biogenesis of *Arabidopsis thaliana* elongating cells: transcriptomics complements proteomics. BMC Genomics 10: 505

Jones L, Milne JL, Ashford D, McQueen-Mason SJ (2003) Cell wall arabinan is essential for guard cell function. Proc Natl Acad Sci U S A 100: 11783–11788

Kong Y, Peña MJ, Renna L, Avci U, Pattathil S, Tuomivaara ST, Li X, Reiter WD, Brandizzi F, Hahn MG, Darvill AG, York WS, O'Neill MA (2014) Galactose-depleted xyloglucan is dysfunctional and leads to dwarfism in *Arabidopsis*. Plant Physiol 167: 1296–1306

Kong G, Wan L, Deng YZ, Yang W, Li W, Jiang L, Situ J, Xi P, Li M, Jiang Z (2019) Pectin acetylesterase PAE5 is associated with the virulence of plant pathogenic oomycete *Peronophythora litchii*. Physiol Mol Plant Path 106: 16–22

Lampugnani ER, Khan GA, Somssich M, Persson S (2018) Building a plant cell wall at a glance. J Cell Sci 131: jcs207373

Leroux C, Bouton S, Kiefer-Meyer MC, Fabrice TN, Mareck A, Guénin S, Fournet F, Ringli C, Pelloux J, Drioich A, Lerouge P, Lehner MJC (2015) Pectin methylesterase48 is involved in *Arabidopsis* pollen grain germination. Plant Physiol 167: 367–380

Levesque-Tremblay G, Pelloux J, Braybrook SA, Müller K (2015) Tuning of pectin methylesterification: consequences for cell wall biomechanics and development. Planta 242: 791–811

López-Calcagno PE, Abuzaid AO, Lawson T, Raines CA (2017) *Arabidopsis* CP12 mutants have reduced levels of phosphoribulokinase and impaired function of the Calvin-Benson cycle. J Exp Bot 68: 2285–2298

McKenna BA, Kopittke PM, Wehr JB, Blamey FPC, Menzies NW (2010) Metal ion effects on hydraulic conductivity of bacterial cellulose–pectin composites used as plant cell wall analogs. Physiol Plant 138: 205–214

Mertz RA, Olek AT, Carpita NC (2012) Alterations in cell-wall glycosyl linkage structure of *Arabidopsis* murus mutants. Carbohydr Polym 89: 331–339

Moore JP, Farrant JM, Driouich A (2008) A role for pectin-associated arabinans in maintaining the flexibility of the plant cell wall during water deficit stress. Plant Signal Behav 3: 102–104

Müller K, Levesque-Tremblay G, Bartels S, Weitbrecht K, Wormit A, Usadel B, Haughn G, Kermode AR (2013) Demethylesterification of cell wall pectins in *Arabidopsis* plays a role in seed germination. Plant Physiol 161: 305–316
Niinemets Ü, Cescatti A, Rodeghiero M, Tosens T (2005) Leaf internal diffusion conductance limits photosynthesis more strongly in older leaves of Mediterranean evergreen broad-leaved species. Plant Cell Environ 28: 1552–1566
Onoda Y, Wright IJ, Evans JR, Hikosaka K, Kitajima K, Niinemets Ü, Poorter H, Tosens T, Westoby M (2017) Physiological and structural tradeoffs underlying the leaf economics spectrum. New Phytol 214: 1447–1463
Orfila C, Dal Degan F, Jorgensen B, Scheller HV, Ray PM, Ulvskov P (2012) Expression of mung bean pectin acetyl esterase in potato tubers: effect on acetylation of cell wall polymers and tuber mechanical properties. Planta 236: 185–196
Palin R, Geitmann A (2012) The role of pectin in plant morphogenesis. Biosystems 109: 397–402
Parre E, Geitmann A (2005) Pectin and the role of the physical properties of the cell wall in pollen tube growth of *Solanum chacoense*. Planta 220: 582–592
Peaucelle A, Louvet R, Johansen JN, Höfte H, Laufs P, Pelloux J, Mouille G (2008) *Arabidopsis* phyllotaxis is controlled by the methylesterification status of cell-wall pectins. Curr Biol 18: 1943–1948
Peaucelle A, Braybrook SA, Le Guillou L, Bron E, Kuhlemeier C, Höfte H (2011) Pectin-induced changes in cell wall mechanics underlie organ initiation in *Arabidopsis*. Curr Biol 21: 1720–1726
Peguero-Pina JJ, Sancho-Knapik D, Gil-Pelegrín E (2017) Ancient cell structural traits and photosynthesis in today's environment. J Exp Bot 68: 1389–1392
Pelletier S, Van Orden J, Wolf S, Vissenberg K, Delacourt J, Ndong YA, Pelloux J, Bischoff V, Urbain A, Mouille G, Lemonnier G, Renou JP, Höfte H (2010) A role for pectin de-methylesterification in a developmentally regulated growth acceleration in dark-grown *Arabidopsis* hypocotyls. New Phytol 188: 726–739
Pelloux J, Rustérucci C, Mellerowicz EJ (2007) New insights into pectin methylesterase structure and function. Trends Plant Sci 12: 267–277
Peña MJ, Ryden P, Madson M, Smith AC, Carpita NC (2004) The galactose residues of xyloglucan are essential to maintain mechanical strength of the primary cell walls in Arabidopsis during growth. Plant Physiol 134: 443–451
Philippe F, Pelloux J, Rayon C (2017) Plant pectin acetylesterase structure and function: new insights from bioinformatic analysis. BMC Genomics 18: 456
Pooper ZA, Tuohy MG (2010) Beyond the green: understanding the evolutionary puzzle of plant and algal cell walls. Plant Physiol 153: 373–383
Remoroza C, Wagenknecht M, Gu F, Buchholt HC, Moerschbacher BM, Schols H, Gruppen H (2014) A *Bacillus licheniformis* pectin acetylesterase is specific for homogalacturonan acetylated at O-3. Carbohydr Polym 107: 85–93
Roig-Oliver M, Nadal M, Clemente-Moreno MJ, Bota J, Flexas J (2020) Cell wall components regulate photosynthesis and leaf water relations of *Vitis vinifera* cv. Grenache acclimated to contrasting environmental conditions. J Plant Physiol 244: 153084
Rui Y, Dinnery JR (2019) A wall with integrity: surveillance and maintenance of the plant cell wall under stress. New Phytol 225: 1428–1439
Scheler C, Weitbrecht K, Pearce SP, Hampstead A, Büttner-Mainik A, Lee KJD, Voegele A, Oracz K, Dekkers BJW, Wang X, Wood ATA, Bentsink L, King JR, Knox JP, Holdsworth MJ, Müller K, Leubner-Metzger G (2015) Promotion of testa rupture during garden cress germination involves seed compartment-specific expression and activity of pectin methylesterases. Plant Physiol 167: 200–215
Sénéchal F, Graff L, Surcouf O, Marcelo P, Rayon C, Bouton S, MAreck A, Mouille G, Stintzi A, Höfte H, Lerouge P, Schaller A, Pelloux J (2014) *Arabidopsis* PECTIN METHYLESTERASE17 is co-expressed with and processed by SBT3.5, a subtilisin-line serine protease. Ann Bot 114: 1161–1175
Solecka D, Zebrowski J, Kacperska A (2008) Are pectins involved in cold acclimation and de-acclimation of winter oil-seed rape plants? Ann Bot 101: 521–530
Sørensen I, Domozych D, Williats WGT (2010) How have plant cell walls evolved? Plant Physiol 153: 366–372
Tenhaken R (2015) Cell wall remodelling under abiotic stress. Front Plant Sci 5: 771
Terashima I, Miyazawa SI, Hanba YT (2001) Why are sun leaves thicker than shade leaves? Consideration based on analyses of CO_2 diffusion in the leaf. J Pl Res 114: 93–105
Tomás M, Flexas J, Copolovici L, Galmés J, Hallik L, Medrano H, Ribas-Carbó M, Tosens T, Vislap V, Niinements Ü (2013) Importance of leaf anatomy in determining mesophyll diffusion conductance to CO_2 across species: quantitative limitations and scaling up by models. J Exp Bot 64: 2269–2281
Tosens T, Nishida K, Gago J, Coopman RE, Cabrera HM, Carriquí M, Laanisto L, Morales L, Nadal M, Rojas R, Talts E, Tomás M, Hanba Y, Niinemets Ü, Flexas J (2016) The photosynthetic capacity in 35 ferns and fern allies: mesophyll CO_2 diffusion as a key trait. New Phytol 209: 1576–1590
Turbant A, Fournet F, Lequart M, Zabijak L, Pageau K, Bouton S, Wuytswinkel V (2016) PME58 plays a role in pectin distribution during seed coat mucilage extrusion through homogalacturonan modification. J Exp Bot 67: 2177–2190
Valentini R, Epron D, Angelis PD, Matteucci G, Dreyer E (1995) In situ estimation of net CO_2 assimilation, photosynthetic electron flow and photorespiration of

Turkey oak (*Q. cerris* L.) leaves: diurnal cycles under different water supply. Plant Cell Environ 18: 631–664
Veromann-Jürgenson LL, Tosens T, Laanisto L, Niinemets Ü (2017) Extremely thick cell walls and low mesophyll conductance: welcome to the world of ancient living! J Exp Bot 68: 1639–1653
Weraduwage SM, Kim SJ, Renna L, Anozie FC, Sharkey TD, Brandizzi F (2016) Pectin methylesterification impacts the relationship between photosynthesis and plant growth in *Arabidopsis thaliana*. Plant Physiol 171: 833–848
Whitney SM, Houtz RL, Alonso H (2011) Advancing our understanding and capacity to engineer nature's CO_2-sequestering enzyme, Rubisco. Plant Physiol 155: 27–35
Zhang R, Hu H, Wang Y, Hu Z, Ren S, Li J, He B, Wang Y, Xia T, Chen P, Xie G, Peng L (2020) A novel rice *fragile culm 24* mutant encodes a UDP-glucose epimerase that affects cell wall property and photosynthesis. J Exp Bot 71: 2956–2969. https://doi.org/10.1093/jxb/eraa044
Zhao X, Liu N, Shang N, Zeng W, Ebert B, Rautengarten C, Zeng QY, Li H, Chen X, Beahan C, Bacic A, Heazlewood JL, Wu AM (2018) Three UDP-xylose transporters participate in xylan biosynthesis by conveying cytosolic UDP-xylose into the Golgi lumen in *Arabidopsis*. J Exp Bot 69: 1125–1124

Supporting information

Additional supporting information may be found online in the Supporting Information section at the end of the article.

Table S1. Anatomical characterization from semi-fine cross-sections of *Arabidopsis thaliana* Col-0, *atpae11.1* and *atpme17.2* genotypes.

Fig. S1. Net CO_2 assimilation at different CO_2 concentrations at the sub-stomatal cavity (A_N-C_i curves) of *Arabidopsis thaliana* Col-0, *atpae11.1* and *atpme17.2* genotypes.

Edited by R. Rivero